

1 **Defining Flood Seasons Globally using Temporal**  
2 **Streamflow Patterns**

3 **Donghoon Lee<sup>1</sup>, Philip Ward<sup>2</sup> and Paul Block<sup>1</sup>**

4 [1]{University of Wisconsin - Madison, Madison, Wisconsin, USA}

5 [2]{Institute for Environmental Studies (IVM), VU University Amsterdam, the Netherlands}

6 Corresponding Author: Paul Block (paul.block@wisc.edu)

1 **Abstract**

2 Globally, flood catastrophes lead all natural hazards in terms of impacts on society, causing  
3 billions of dollars of damages annually. Here, a novel approach to defining flood seasons  
4 globally is presented by identifying temporal patterns of streamflow objectively. The main  
5 flood season is identified using a volume-based threshold technique and the PCR-GLOBWB  
6 model. In comparison with observations, 40% (50%) of locations at a station (sub-basin) scale  
7 have identical peak months and 81% (89%) are within 1 month, indicating strong agreement  
8 between modeled and observed flood seasons. Model defined flood seasons are additionally  
9 found to well represent actual flood records from the Dartmouth Flood Observatory, further  
10 substantiating the models ability to reproduce the appropriate flood season. Minor flood  
11 seasons are also defined for bi-modal flood regimes. This is especially attractive for regions  
12 with limited observations and/or little capacity to develop early warning flood systems. The  
13 temporal patterns of global streamflow identified can lead to improved understanding of flood  
14 frequency, trends, and inter-annual variability and further benefit flood risk planning and  
15 preparation efforts.

# 1 **1 Introduction**

2 Flood disasters rank as one of the most destructive natural hazards in terms of economic  
3 damage, causing billions of dollars of damage each year (Munich Re, 2012.) These flood  
4 damages have risen starkly over the past half-century given the rapid increase in global  
5 exposure (Bouwer, 2011; UNISDR, 2011; Visser et al., 2014.) To specifically address flood  
6 disasters from a global perspective, understanding of global-scale flood processes and  
7 streamflow variability is important (Dettinger and Diaz, 2000; Ward et al., 2014). In recent  
8 decades, studies have investigated global-scale streamflow characteristics using observed  
9 streamflow from around the world (Beck et al., 2013; McMahon, 1992; McMahon et al.,  
10 2007; Peel et al., 2001, 2004; Poff et al., 2006; Probst and Tardy, 1987) and modeled  
11 streamflow from global hydrological models (Beck et al., 2015; van Dijk et al., 2013; McCabe  
12 and Wolock, 2008; Milly et al., 2005; Ward et al., 2013, 2014) to investigate ungauged and  
13 poorly gauged basins (Fekete and Vörösmarty, 2007). Despite this broad attention on annual  
14 streamflow and its connections to global climate processes and precursors, there has been  
15 relatively little attention paid to the intra-annual timing of streamflow, emphasizing the need  
16 for analysis of seasonal streamflow patterns to further improve understanding of large-scale  
17 hydrology and atmospheric behaviors on the main (flood) streamflow season globally  
18 (Dettinger and Diaz, 2000). Moreover, better assessment of streamflow timing and seasonality  
19 is important for addressing frequency and trend analyses, flood protection and preparedness,  
20 climate-related changes, and other hydrological applications that possess important sub-  
21 annual characteristics (Burn and Arnell, 1993; Burn and Hag Elnur, 2002; Cunderlik and  
22 Ouarda, 2009; Hodgkins et al., 2003). This motivates further investigation of intra-annual  
23 temporal streamflow patterns globally.

24 Only a small number of studies have investigated global-scale seasonality and temporal  
25 patterns of streamflow, with minimal focus on objective streamflow timing. Haines et al.  
26 (1988) cluster 969 world rivers into 15 categories based on seasonality and average monthly  
27 streamflow data, and present one of the first maps providing a global classification. Burn and  
28 Arnell (1993) aggregate 200 streamflow stations into 44 similar climatic regions and  
29 subsequently combine these into 13 groups using hierarchical clustering based on similarity of  
30 the annual maximum flow index, providing spatial and temporal coincidences of flood  
31 response. Dettinger and Diaz (2000) aggregate 1345 sites into 10 clusters based on seasonality

1 using climatological fractional monthly flows (CFMFs) to identify peak months and linkages  
2 with large-scale climate drivers.

3 In general, these studies define key seasons based on large-scale drivers/patterns and  
4 clustering, and describe annual peak timing based on streamflow amplitude. The clustering  
5 approach employed, however, tends to lump many smaller basins together into one major  
6 season, and may not be representative of local scale conditions, especially for those basins at  
7 the margins of the clusters where streamflow patterns may not have a single defined major  
8 season (e.g. perpetually wet or dry, bi-modal, etc.) In lieu of large-scale clustering and  
9 aggregation, we propose addressing basins (and even grid cells) individually, in a  
10 disaggregated fashion. Additionally, as an alternative to simply using the annual maximum  
11 streamflow amplitude to define the annual peak timing, we consider a volumetric approach  
12 based on surpassing a predefined threshold at the daily scale to define peak streamflow timing.  
13 Both of these advancements are conditioned on an objective approach to define major and  
14 minor flood seasons globally. Parsing out these peak seasons – if they exist – can improve  
15 flood characterization, leading to better understanding of flood potential, causation, and  
16 management, particularly in ungauged or limited-gauged basins.

17

## 18 **2 Data description**

### 19 **2.1 Streamflow stations**

20 Daily streamflow observations utilized in this study are from the Global Runoff Data Centre  
21 ([GRDC, 2007](#)), specifically those, stations located along the global hydrology model's  
22 drainage network. Since station records that are missing even short periods may effect how a  
23 flood season is defined, we have excluded years with any daily missing values. In this study, a  
24 minimum of 20 hydrological years is required for a station to be retained, leaving, 691  
25 stations from all continents except Antarctica, with upstream basin areas ranging from 9,539  
26 to 4,680,000 km<sup>2</sup> and periods of record between 20 - 43 years across 1958 - 2000 (Figure 1.)  
27 Although this criteria is admittedly quite strict (no missing daily data), relaxing the criteria  
28 does not add a significant number of stations.

## 1   **2.2 PCR-GLOBWB**

2   In this study, we evaluate simulations of daily streamflow over the period 1958-2000 taken  
3   from [Ward et al. \(2013\)](#), carried out using PCR-GLOBWB (PCRaster GLOBal Water  
4   Balance), a global hydrological model with a 0.5° x 0.5° resolution ([Van Beek and Bierkens,](#)  
5   [2009](#); [Van Beek et al., 2011](#).) Although the PCR-GLOBWB model is not calibrated, and  
6   simulations may contain biases and uncertainty at coarse spatial resolution, the long time-  
7   series of streamflow provided globally has been deemed sufficient to estimate long-term flow  
8   characteristics with spatial consistency ([Winsemius et al., 2013](#)). Additionally, this model has  
9   been validated in previous studies in terms of streamflow ([Van Beek et al., 2011](#)), terrestrial  
10   water storage ([Wada et al., 2011](#)) and extreme discharges ([Ward et al., 2013](#)), with strong  
11   model performance. Note that for the simulations used in this study, the maximum storage  
12   within the river channel is based on geomorphological laws that do not account for existing  
13   flood protection measures such as dikes and levees.

14   For the simulations used in this study, the PCR-GLOBWB model was forced with daily  
15   meteorological data from the WATCH (Water and Global Change) project ([Weedon et al.,](#)  
16   [2011](#)), namely precipitation, temperature, and global radiation data. These data are available  
17   at the same resolution as the hydrological model (0.5° x 0.5°.) The WATCH forcing data were  
18   originally derived from the ERA-40 reanalysis product ([Uppala et al., 2005](#)), and were  
19   subjected to a number of corrections including elevation, precipitation gauges, time-scale  
20   adjustments of daily values to reflect monthly observations, and varying atmospheric aerosol-  
21   loading. It is possible that this may have some minor effect on streamflow simulation, likely  
22   providing more realistic outcomes. Full details of corrections are described in [Weedon et al.](#)  
23   [\(2011\)](#).

24

## 25   **3 Defining flood seasons**

26   To identify spatial and temporal patterns of dominant streamflow uniformly, we design a  
27   fixed time window for representing flood seasons globally. Here we define major flood  
28   seasons as the 3-month period most likely to contain dominant streamflow and the annual  
29   maximum flow. The central month is referred to as the Peak Month (PM) and the full 3-month  
30   period is referred to as the Flood Season (FS.) Specifically, we define PM first, and then  
31   define FS as the period also containing the month before and after the PM. This approach is

1 performed for both observed (station) and simulated (model) streamflow to gauge  
2 performance.

### 3 **3.1 Methodology for defining grid-cell scale flood seasons**

4 In the last few decades, a number of studies have investigated the timing of floods in the  
5 context of analyzing seasonality, frequency and trends. Generally, two main factors are  
6 emphasized regarding flood timing: streamflow volume and streamflow magnitude. For  
7 streamflow volume an occurrence date is commonly recorded, often in the context of trend  
8 analysis. For examples, [Hodgkins and Dudley \(2006\)](#) use winter-spring center of volume  
9 (WSCV) dates to analyze trends in snowmelt-induced floods, and [Burn \(2008\)](#) uses percentile  
10 of annual streamflow volume dates as indicators of flood timing, also for trend analysis. The  
11 second factor (streamflow magnitude) is traditionally more focused on peak-flood timing.  
12 Two sampling methods are frequently applied in hydrology. The first and most common is the  
13 annual-maximum (AM) method, which samples the largest streamflow in each year. The  
14 second method is the peaks-over-threshold (POT) method ([Smith, 1984, 1987; Todorovic and  
15 Zelenhasic, 1970](#)), in which all distinct, independent dominant peak flows greater than a fixed  
16 threshold are counted, prior to a specified date. In contrast to the AM method, this threshold  
17 characteristic can capture multiple large independent floods within a single year, including the  
18 annual maximum flow, but may also miss the annual maximum flow in years in which  
19 streamflow is less than the pre-defined threshold ([Cunderlik et al., 2004a](#)) Thus, deciding the  
20 proper threshold level is important. Therefore, to define the FS, and specifically the PM, both  
21 volume and magnitude aspects need to be considered ([Javelle et al. 2003](#)). To do this, we  
22 adopt a volume-based threshold technique. This technique is similar to a streamflow volume-  
23 based method in terms of capturing the Julian day by which a fixed percentage of the annual  
24 streamflow volume has occurred ([Burn, 2008](#)), however it also applies this fixed percentage  
25 across the entire streamflow record and records points where streamflow volume surpasses it,  
26 drawing from the prescribed threshold concept in the POT method. Here we select streamflow  
27 surpassing the top 5% of the flow duration curve (FDC) across all years (1958-2000) as the  
28 threshold for considering a high streamflow level, as commonly adopted in threshold  
29 approaches ([Burn, 2008; Mishra et al., 2011.](#)) The month containing the greatest number of  
30 occurrences in the top 5% is defined as the PM, and subsequently the FS is defined as the  
31 period containing the PM plus the month before and after the PM. Figure 2 provides an  
32 example based on seven years of synthetic streamflow; the number of days surpassing the 5%

1 threshold is listed for each month. In this example, August has the largest number of days  
2 over the threshold (105 days), thus August is defined as PM and July-September is defined as  
3 FS.

4 To evaluate the defined FS objectively, by evaluating the number of annual maximum flows  
5 captured, we develop a simple evaluating statistic called the Percentage of Annual Maximum  
6 Flow (PAMF). PAMF is computed as shown in Eq. 1:

$$7 \quad PAMF(i) = \frac{\sum_{j=i-1}^{i+1} n_{AMF}(j)}{\sum_{k=1}^{12} n_{AMF}(k)}, \quad 1 \leq i \leq 12 \quad (1)$$

8 where  $n_{AMF}(i)$  denotes the number of annual maximum flows that occur in month  $i$  across  
9 the full record. In Eq. (1), when  $i$  is 1 (Jan),  $i - 1$  in the summation is 12 (Dec), and when  $i$  is  
10 12 (Dec),  $i + 1$  is 1 (Jan). Here the PAMF provides the percent of time the annual maximum  
11 flows occurs in the defined FS across the evaluation period. The PAMF is relatively simple,  
12 yet inherently contains magnitude and volume properties of streamflow. For example, a high  
13 PAMF indicates that the FS is highly likely to contain the annual maximum flood each year.  
14 In contrast, a low PAMF indicates that the timing of the annual maximum flow is more likely  
15 to vary temporally, and may be a result of bimodal seasonality, consistently high or low  
16 streamflow throughout the year, streamflow regulated by infrastructure or natural variation. In  
17 this study, we subjectively classify FS PAMF values as: high = 80-100%, low = 60-80%, and  
18 poor = 40-60%. The PAMF is calculated for both the observed streamflow at the selected 691  
19 GRDC stations and the simulated streamflow at the associated 691 grid locations.

20 Clearly the volume-based threshold method is not the only available classification technique  
21 for defining the PM. To gauge its performance, the AM method and other volume methods  
22 with different given durations are selected for comparison, namely  $Q_{AM}$ ,  $Q_{7day}$ ,  $Q_{15day}$  and  
23  $Q_{30day}$ . For the  $Q_{AM}$  approach, which is based on the AM method, the FS is simply centered  
24 on the PM containing the largest number of annual maximum flow occurrences across the  
25 total years available. The  $Q_{7day}$  approach defines the PM as the month with maximum  
26 streamflow volume during any seven consecutive day period; the month with the most periods  
27 across all years becomes the PM for the defined FS. The  $Q_{15day}$  and  $Q_{30day}$  approaches are  
28 similar to the  $Q_{7day}$  approach, respectively using 15 and 30 days consecutively.  
29 Comparitavely, the flow-based classification techniques with a shorter time component (1-7  
30 days) favor identifying flood magnitude while the techniques with longer time components

1 (15-30 days) favor identifying flood volume. The volume-based threshold method is an  
2 attempt to bridge these two criteria.

3 Cross-correlations of PM between the volume-based threshold technique and other  
4 classification techniques are quite similar (0.87-0.90; Table 1), preliminarily indicating some  
5 success in capturing both magnitude and volume. The PAMF is also useful for comparing  
6 classification techniques' performance when they define PM differently at the same location.  
7 This occurs at 45% of stations and 40% of associated grids for observed and modeled  
8 streamflow, respectively. The classification technique having the highest PAMF most often  
9 for those stations or grids may be considered slightly superior in terms of containing more  
10 annual maximum flows in their defined FSs. The volume-based threshold technique has the  
11 highest PAMF values by at least 2% of grids (1% of stations) more than any other technique  
12 for modeled (observed) streamflow. Finally, classification technique performance may be  
13 evaluated by comparing the temporal difference (number of months) between model-based  
14 and observed PMs; closer is clearly superior. Overall the volume-based threshold technique  
15 produces a greater degree of similarity between model-based and observed PMs (2-5% higher  
16 in  $\pm 1$  month difference and 1-5% higher in  $\pm 2$  month difference.) Based on these findings, the  
17 remainder of the analysis is carried out utilizing the volume-based threshold technique only.

### 18 **3.2 Methodology for defining sub-basin scale flood seasons**

19 In addition to evaluating the FS at the 691 grid cells based on model outputs, the PM and FS  
20 can also be defined at the sub-basin scale globally where observations are present. Previous  
21 studies have investigated flood seasonality as it relates to basin characteristics; for example,  
22 basins are delineated/regionalized and grouped according to similarity/dissimilarity of  
23 streamflow seasonality (Burn, 1997; Cunderlik et al., 2004a), or conversely, flood seasonality  
24 is occasionally used to assess hydrological homogeneity of a group of regions (Cunderlik and  
25 Burn, 2002; Cunderlik et al., 2004b), thus evaluating at the sub-basin scale is warranted.

26 While defining a single PM for a large-scale basin may be convenient, it may be difficult to  
27 justify given the potentially long travel times and varying climate, topography, vegetation, etc.  
28 Additionally, infrastructure may be present to regulate flow for flood control, water supply,  
29 irrigation, recreation, navigation, and hydropower (WCD, 2000), causing managed and natural  
30 flow regimes to differ drastically. This becomes important, as globally more than 33,000  
31 records of large dams and reservoirs are listed (ICOLD, 1998-2009), with geo-referencing



1 available for 6,862 of them (Lehner et al., 2011). Nearly 50% of large rivers with average  
2 streamflow in excess of 1,000 m<sup>3</sup>/s are significantly modulated by dams (Lehner et al., 2011),  
3 often significantly attenuating flow hydrographs and flood volumes. The PAMF, as  
4 previously defined, can aid in identifying stations affected by upstream reservoirs through low  
5 PAMF values. This is applied with the assumption that reservoir flood control disperses the  
6 annual maximum flows across months rather concentrated within a few months (e.g. akin to  
7 natural flow.) In this study, we used the global sub-basins from the 30' global drainage  
8 direction map (DDM30) dataset (Döll and Lehner, 2002) with separation of large basins  
9 (Ward et al., 2014).

10 To define a sub-basin's PM, the maximum PAMF and associated PM for each station within  
11 the sub-basin are considered according to the following:

- 12 • If multiple stations exist within the sub-basin, the PM is defined as the PM occurring  
13 for the largest number of stations
- 14 • If there is a tie between months, their average PAMF values are compared, and the  
15 month having the higher average PAMF is defined as the PM.
- 16 • If there is a tie between months and equivalent average PAMF values, the month  
17 having the higher average annual streamflow is defined as the PM.

18 The sub-basin's PM is defined based on the occurrence of station or grid-level PMs rather  
19 than the PAMF values to diminish results being skewed by biased simulations or varying  
20 climate effects in small parts of the sub-basin. When there are an equal number of occurrences  
21 for different PMs, the average PAMF values are used to determine which PM is selected. In  
22 this case, the effect of stations downstream of reservoirs will be minimized given their  
23 typically low average PAMF values. This procedure is applied for both stations (observations)  
24 and corresponding grid cells (model) in each sub-basin. To illustrate, consider the 6 GRDC  
25 stations in the Zambezi River Basin (Figure 3.) For most of the stations, the observed PM is  
26 defined as a month later than the model-based PM (Table 2), an apparent bias in the model.  
27 The PAMF of STA06 observations is noticeably lower than for other stations (36%; Table 2)  
28 given its location downstream of the Itzhi-Tezhi dam (STA05) (Figure 3.) Otherwise, PAMF  
29 values are consistently high across all stations. March is the PM identified most often, thus the  
30 final sub-basin PM selected is March.

31 In contrast, the model-based simulated streamflow produces a high PAMF at STA06 (97%),  
32 as the Itzhi-Tezhi dam is not represented in the simulations used for this study, and

1 subsequently does not account for modulated streamflow. Across other stations, the PAMF is  
2 also high, however an equal number of stations select February and March. In this case,  
3 February is selected as the final basin PM given its higher average PAMF value (96% vs.  
4 91%.)

5 By this approach, all 691 GRDC stations are grouped into 223 sub-basins to define the PM  
6 (Figure 6.); 58% of sub-basins are defined by a single station, only 7.6% (observations) and  
7 8.1% (model) of sub-basins have ties when defining PMs, and only one sub-basin has a tie  
8 between PMs and average PAMF values.

9

## 10 **4 Verification of selected flood seasons**

11 Model-based PMs are verified by comparing with observation-based PMs at station and sub-  
12 basin scales. Additionally, historic flood records from the Dartmouth Flood Observatory  
13 (DFO) are used to compare basin-level PMs to actual flooded areas spatially and temporally.  
14 Specifically, we apply the following information from DFO: start time, end time, duration and  
15 geographically estimated area at 3,486 flood records across 1985-2008.

### 16 **4.1 Observed versus modeled flood seasons**

17 Ideally the model-based and observed GRDC stations have fully or partially overlapping FS  
18 periods. If so, this builds confidence in interpreting FSs at locations where no observed data  
19 are available. For comparing modeled PMs to observations, the defined PMs and calculated  
20 PAMF are represented globally at the station scale (Figure 4-5) and sub-basin scale (Figure 6)  
21 with temporal differences of PMs (modeled PM – observed PM). These temporal differences  
22 are also compared at the continental scale (Figure 7.) For example, in the United States and  
23 Canada, 38% of stations and 51% of sub-basins produce identical PMs, growing to 82% of  
24 stations and 93% of sub-basins when considering a  $\pm 1$  month temporal difference (e.g. FS;  
25 Figure 7.) GRDC stations in the southeastern United States express relatively lower PAMF  
26 values for observations (40-60%) than model outputs (60-80%), due to the high level of  
27 managed infrastructure. In the central United States and Europe, low PAMF values are  
28 computed for both observation and model outputs (Figure 5) with notable temporal  
29 differences (Figure 4 (c).) This is attributable, at least in part, to reservoirs and dams along the  
30 Mississippi, Missouri and Danube rivers.

1 Globally, comparing model and GRDC data, 40% of the locations share the same PM.  
2 Considering a difference of  $\pm 1$  month, this jumps to 81%, and 91% for  $\pm 2$  months (Figure 7.)  
3 From a sub-basin perspective, the similarities are even stronger (50% identical PM, 88%  $\pm 1$   
4 month and 92%  $\pm 2$  month), indicating a relatively high level of agreement. For locations  
5 having dissimilar PMs ( $\geq \pm 3$  months, 9% of locations and 8% of sub-basins), a substantial  
6 portion are located downstream of reservoirs directly, such as STA06 in the Zambezi example  
7 (Table 1), or are low-flow (dry) locations, both producing exceedingly low PAMF values.  
8 Differences in PMs are not unexpected for low-flow locations, given the propensity for the  
9 annual streamflow maximum to potentially occur in a wide number of months. Overall,  
10 however, as more than 80% of both stations and sub-basins have similar PMs ( $\pm 1$  month), it  
11 appears that the global water balance model performs appropriately well in defining flood  
12 seasons globally at locations where observations are available.

13 This may be subsequently extended to defining PMs and PAMF at all grid cells (Figures 8-9.)  
14 Generally, a low PAMF indicates an unstable annual maximum flow, which occurs in cases of  
15 constant-flow, low-flow, bi-modal flow and regulated flow. All cases, except regulated flow,  
16 are simulated within the PCR-GLOBWB simulations used, thus the cell-based PAMF values  
17 (Figure 9) can provide a sense of confidence for the defined PM (Figure 8.) Examples of low-  
18 flow regions include the central United States and Australia having low PAMF regional  
19 values (Figure 9.) Bi-modal regions, such as much of East Africa with its two rainy seasons,  
20 may also be associated with low PAMF values.

## 21 **4.2 Modeled flood seasons versus actual flood records**

22 Model-based PMs may also be verified (subjectively) by surveying historic flood records.  
23 One such source is the Dartmouth Flood Observatory (DFO), a large, publically accessible  
24 repository of major flood events globally over 1985-2008, based on media and governmental  
25 reports and instrumental and remote sensing sources. Delineations of affected areas are best  
26 estimates (Brakenridge, 2011.) The DFO records provide duration of each flooding event, as  
27 defined by the report or source, and represented as occurrence month (Figure 10.) DFO flood  
28 events and grid cell based PMs (Figure 8) may be compared outright, however their  
29 characteristics differ slightly. The DFO covers 1985-2008 while the model represents 1958-  
30 2000. Also, the model-based PM represents the month most likely for a flood to occur; the  
31 DFO is simply a reporting of when the event did occur, regardless of whether it fell in the  
32 expected flood season or not. Nevertheless, model-based PMs and historic flooding records

1 illustrate a striking similarity (compare Figures 8 and 10), further supporting the model's  
2 ability to appropriately identify the PM spatially. Consistently, regions with high model-based  
3 PAMF (80-100%), such as Eastern South America, Central Africa and Central Asia, tend to  
4 agree well with DFO records, while poor or less than poor PAMF (0-60%) regions, such as  
5 Central North America, Europe, and East Africa, tend not to be in agreement with DFO  
6 records. In these low PAMF regions, however, DFO records also illustrate floods occurring  
7 sporadically throughout the year, further supporting accordance between cell-based PAMF  
8 and DFO records (Figures 9 and 10.)

9

## 10 **5 Defining minor flood seasons**

11 In some climatic regions, there is no one single, well-defined flood season. For example, East  
12 Africa has two rainy seasons, the major season from June to September and the minor season  
13 from January to April/May. These two seasons are induced by northward and southward shifts  
14 of the inter-tropical convergence zone (ITCZ) (Seleshi and Zanke, 2004.) This bi-modal East  
15 African pattern allows for potential flooding in either season. In Canada, as another example,  
16 the dominant spring snowmelt season (Mar-May) and fall rainy season (Aug-Oct) allow for  
17 flood occurrences in either period (Cunderlik and Ouarda, 2009.)

18 Previous studies have investigated techniques to differentiate seasonality from uni-, bi- and  
19 multi-modal streamflow climatologies and evaluate trends in timing and magnitude of  
20 streamflow, including the POT method, directional statistics method, and relative flood  
21 frequency method (Cunderlik and Ouarda, 2009; Cunderlik et al., 2004a). These methods may  
22 perform well at the local (case-specific) scale to define minor flood seasons, however  
23 applying them uniformly at the global scale can be problematic, given spatial heterogeneity.  
24 Additionally, even though bimodal streamflow climatology may be detected, the magnitude of  
25 streamflow in the minor season may or may not be negligible in regards to flooding potential  
26 as compared with the major season.

27 To detect noteworthy minor flood seasons globally, we classify streamflow regimes by  
28 climatology and monthly PAMF value, calculated using Eq. (1) at each month (Figure 11.)  
29 Classifications include unimodal, bimodal, constant, and low-flow. The unimodal streamflow  
30 climatology has high values of PAMF around the PM; the bi-modal classification is  
31 represented by two peaks of PAMF (and may therefore contain a minor season); both constant  
32 and low-flow classifications represent low values of PAMF between months. Distinguishing

1 between bi-modal and other classifications is nontrivial. For example, initial inspection of the  
2 constant streamflow classification (both climatology and monthly PAMF, Figure 11 (c)) could  
3 be mistaken for a non-dominant bi-modal distribution. We adopt the following criteria to  
4 differentiate bi-modal streamflow from uni-modal, constant, and low-flow conditions.

- 5 • The low-flow classification is defined for annual average streamflow less than 1  
6  $\text{m}^3/\text{sec}$ .
- 7 • The major and minor PMs must be separated by at least two months in order to  
8 prevent an overlap of each FS (3-month.)
- 9 • If there is a peak in the monthly PAMF values outside the major FS, it is regarded as a  
10 *potential* minor PM. If the sum of the major and *potential* minor PM's PAMF is  
11 greater than 60% (minimum of 29 out of 43 annual maximums fall in one of the FS),  
12 the *potential* minor PM is confirmed as a minor PM; the major PM's PAMF cannot  
13 exceed 80%.

14 A *potential* minor PM is identified by a secondary peak in the monthly PAMF rather than the  
15 magnitude or shape of streamflow. A minor FS is not defined when a major PM's PAMF is  
16 greater than 80% (minimum of 35 out of 43 annual maximums), indicating a robust uni-modal  
17 streamflow character (Figure 11 (a)). The sum of both major and minor PM's PAMF (joint  
18 PAMF) is used to determine the likelihood that one of the FSs contains the annual maximum  
19 flow; a high value of the joint PAMFs (80-100%) indicates strong likelihood (Figure 11 (b)),  
20 moderate values (60-80%) imply moderate likelihood, with some probability of being  
21 classified as constant streamflow (Figure 11 (c)); low values (40-60%) are likely constant or  
22 low streamflow (Figure 11 (d)). Minor FSs are similar to major FSs, containing the minor PM  
23 and the month before and after. Minor FSs are evident in the tropics and sub-tropics and are  
24 spatially consistent with bi-modal rainfall regimes discovered by Wang (1994) (Figure 12.)  
25 Examples include East Africa (second rainy season in winter) and Canada (rainfall-dominated  
26 runoff in autumn) both having high joint PAMF values (80-100%.) Additional examples  
27 include the major FS (NDJ) and minor FS (MAM) in Central Africa consistent with the  
28 latitudinal movement of the ITCZ, intra-Americas' major FS (ASON) and minor FS (AMJJ)  
29 (Chen and Taylor, 2002), and coastal regions of British Columbia in Canada and southern  
30 Alaska's minor FS (SOND) due to wintertime migration of the Aleutian low from the central  
31 north Pacific (Figure 12.) Distinct runoff process controlled by different climate and  
32 hydrology systems can induce a bi-modal peak within a large-scale basin, such as the

1 upstream sections of the Yenisey and Lena river systems in Russia where the major FS (AMJ)  
2 is dominated by snowmelt and the minor FS (JAS) is spurred on by the Asian monsoon. The  
3 same mechanism produces minor FSs around the extents of the Asian summer monsoon (90-  
4 100% of sum of PAMFs) (Figure 9 and 12.) Moderate minor FSs include, for example, the  
5 southern United States' (Texas and Oklahoma) bi-modal rainfall pattern (AMJ and SON) and  
6 in the southwestern United States (Arizona) where the summertime major FS (JJA) is  
7 produced by the North American monsoon and the wintertime minor FS (DJF) is affected by  
8 the regional large-scale low pressure system (Woodhouse, 1997). Southeastern Brazil's  
9 summertime major FS (NDJF) and post-summer minor FS (AMJ) are dominated by formation  
10 and migration of the South Atlantic Convergence Zone (Herdies, 2002; Lima and Satyamurty,  
11 2010). In central and eastern Europe, the major FS (FMAM) and minor FS (JJA) are defined  
12 as moderate (60-80% of joint PAMF values for central Europe and 70%-90% for eastern  
13 Europe), indicating that a minor FS is not overly pronounced; for northeastern Europe the  
14 major FS (MAM) and minor FS (NDJ) contain high joint PAMF values (80%-100%.)

15 For the major FS and minor FS with joint PAMF values exceeding 60% (Figure 13), flood  
16 records (DFO) occurring over more than one month are counted in each month based on the  
17 reported duration. Although one distinct flood event may dominate a monthly DFO record,  
18 strong similarity is evident between the FSs and monthly flood records (Figure 13.) Minor  
19 FSs with high PAMF values corresponding well with observed DFO flood records include  
20 East Africa (bi-modal streamflow), the intra-Americas, and Northern Asia; only a few  
21 reported flood records occur in the minor FSs in high latitudes.

22

## 23 **6 Conclusions and Discussion**

24 In this study, a novel approach to defining flood seasons globally is presented by identifying  
25 temporal patterns of streamflow objectively. Simulations of daily streamflow from the PCR-  
26 GLOBWB model are evaluated to define the dominant and minor flood seasons globally. In  
27 order to consider both streamflow magnitude and volume characteristics of floods, a volume-  
28 based threshold technique is applied to define the flood season and subsequently evaluated by  
29 the PAMF. To verify model defined flood seasons, we compare with observations at both  
30 station and sub-basin scales. As a result, 40% of stations and 50% of sub-basins have identical  
31 peak months and 81% of stations and 89% of sub-basins are within 1 month, indicating strong  
32 agreement between model and observed flood seasons. Model defined flood seasons are

1 additionally found to well represent actual flood records from the Dartmouth Flood  
2 Observatory, further substantiating the models ability to reproduce the appropriate flood  
3 season. Regions expressing bi-modal streamflow climatology are also defined to illustrate  
4 potential for noteworthy secondary (minor) flood seasons.

5 Large-scale temporal phenomena associated with the defined major and minor flood seasons  
6 are also identified. For example, global monsoon systems are clearly evident, as driven by the  
7 ITCZ, in central and eastern Africa, Asia and northern South America (Figure 8.) Latitudinal  
8 patterns in the extra-tropics are also quite distinct, with flood seasons often occurring across  
9 similar months in the year. These broad temporal patterns are consistent with previous  
10 findings (e.g. [Burn and Arnell, 1993](#); [Dettinger and Diaz, 2000](#); [Haines et al., 1988](#)), however  
11 this analysis goes further by not being constrained to large-scale patterns for seasonal  
12 definition (via clustering) and also providing a sense of the reliability of the defined flood  
13 seasons. Specifically, the defined PM (Figure 8) has extended [Dettinger and Diaz \(2000\)](#)'s  
14 Peak Months by focusing on basin and grid scale streamflow volumes and providing  
15 likelihood type maps using the PMAF metric developed here (e.g. Figure 9) to represent the  
16 reliability of the defined PM. This can provide a clear sense of whether the identified flood  
17 season is pronounced or vague. The identification of minor flood seasons and deciphering bi-  
18 modal from constant streamflow regimes is another notable contribution of this study; minor  
19 seasons have not been well identified in previous studies. These identified flood seasons are  
20 also consistent with DFO flood records both spatially and temporally, further substantiating  
21 their appropriateness.

22 Although biased simulations may theoretically contribute to a misidentified flood season, the  
23 global hydrological model's ability to well define flood seasons is highlighted in this study.  
24 The full global coverage of streamflow data in the model enables complete flood season  
25 identification globally. This is advantageous for many reasons, including hydrologic  
26 assessment in ungauged and poorly gauged basins and also for investigating flood season  
27 timing within large basins having diverse physical processes, for example, how the PM may  
28 shift along long rivers (e.g. Congo River) or basins with both snowmelt and rain-dominated  
29 processes. These spatially heterogeneous flood seasons at high resolution have the potential to  
30 better characterize streamflow regimes than previous studies (e.g. [Dettinger and Diaz, 2000](#);  
31 [Haines et al., 1988](#)). Additional analysis to include upstream management and regulations is  
32 required to further classify global streamflow regimes and major flood seasons (or the  
33 elimination of them) for specific subbasin-level hydrologic applications.

1

2 *Acknowledgements.* Philip Ward was funded by a VENI grant from the Netherlands  
3 Organisation for Scientific Research (NWO).



## 1 **References**

- 2 Beck, H. E., van Dijk, A. I. J. M., Miralles, D. G., de Jeu, R. A. M., Sampurno Bruijnzeel, L.  
3 A., McVicar, T. R. and Schellekens, J.: Global patterns in base flow index and recession  
4 based on streamflow observations from 3394 catchments, *Water Resour. Res.*, 49(12), 7843–  
5 7863, doi:10.1002/2013WR013918, 2013.
- 6 Beck, H. E., de Roo, A. and van Dijk, A. I. J. M.: Global maps of streamflow characteristics  
7 based on observations from several thousand catchments, *J. Hydrometeorol.*,  
8 150423121816007, doi:10.1175/JHM-D-14-0155.1, 2015.
- 9 Van Beek, L. P. H. and Bierkens, M. F. P.: *The Global Hydrological Model PCR-GLOBWB:  
10 Conceptualization, Parameterization and Verification*, Utrecht., 2009.
- 11 Van Beek, L. P. H., Wada, Y. and Bierkens, M. F. P.: Global monthly water stress: 1. Water  
12 balance and water availability, *Water Resour. Res.*, 47(7), W07517,  
13 doi:10.1029/2010WR009791, 2011.
- 14 Bouwer, L. M.: Have Disaster Losses Increased Due to Anthropogenic Climate Change?, *Bull.*  
15 *Am. Meteorol. Soc.*, 92(1), 39–46, doi:10.1175/2010BAMS3092.1, 2011.
- 16 Brakenridge, G. R.: Global Active Archive of Large Flood Events, Dartmouth Flood  
17 Observatory, University of Colorado. [online] Available from:  
18 <http://floodobservatory.colorado.edu/Archives/index.html>, 2011.
- 19 Burn, D. H.: Catchment similarity for regional flood frequency analysis using seasonality  
20 measures, *J. Hydrol.*, 202(1-4), 212–230, doi:10.1016/S0022-1694(97)00068-1, 1997.
- 21 Burn, D. H.: Climatic influences on streamflow timing in the headwaters of the Mackenzie  
22 River Basin, *J. Hydrol.*, 352, 225–238, doi:10.1016/j.jhydrol.2008.01.019, 2008.
- 23 Burn, D. H. and Arnell, N. W.: Synchronicity in global flood responses, *J. Hydrol.*, 144(1-4),  
24 381–404, doi:10.1016/0022-1694(93)90181-8, 1993.
- 25 Burn, D. H. and Hag Elnur, M. a.: Detection of hydrologic trends and variability, *J. Hydrol.*,  
26 255(1-4), 107–122, doi:10.1016/S0022-1694(01)00514-5, 2002.
- 27 Chen, a. A. and Taylor, M. a.: Investigating the link between early season Caribbean rainfall  
28 and the El Nino+1 year, *Int. J. Climatol.*, 22(1), 87–106, doi:10.1002/joc.711, 2002.
- 29 Cunderlik, J. M. and Burn, D. H.: Local and Regional Trends in Monthly Maximum Flows in  
30 Southern British Columbia, *Can. Water Resour. J.*, 27(2), 191–212, doi:10.4296/cwrj2702191,  
31 2002.
- 32 Cunderlik, J. M. and Ouarda, T. B. M. J.: Trends in the timing and magnitude of floods in  
33 Canada, *J. Hydrol.*, 375(3-4), 471–480, doi:10.1016/j.jhydrol.2009.06.050, 2009.

- 1 Cunderlik, J. M., Ouarda, T. B. M. J. and Bobée, B.: Determination of flood seasonality from  
2 hydrological records / Détermination de la saisonnalité des crues à partir de séries  
3 hydrologiques, *Hydrol. Sci. J.*, 49(3), 511–526, doi:10.1623/hysj.49.3.511.54351, 2004a.
- 4 Cunderlik, J. M., Ouarda, T. B. M. J. and Bobée, B.: On the objective identification of flood  
5 seasons, *Water Resour. Res.*, 40(1), n/a–n/a, doi:10.1029/2003WR002295, 2004b.
- 6 Dettinger, M. D. and Diaz, H. F.: Global Characteristics of Stream Flow Seasonality and  
7 Variability, *J. Hydrometeorol.*, 1(4), 289–310, doi:10.1175/1525-  
8 7541(2000)001<0289:GCOSFS>2.0.CO;2, 2000.
- 9 Van Dijk, A. I. J. M., Peña-Arancibia, J. L., Wood, E. F., Sheffield, J. and Beck, H. E.: Global  
10 analysis of seasonal streamflow predictability using an ensemble prediction system and  
11 observations from 6192 small catchments worldwide, *Water Resour. Res.*, 49(5), 2729–2746,  
12 doi:10.1002/wrcr.20251, 2013.
- 13 Döll, P. and Lehner, B.: Validation of a new global 30-min drainage direction map, *J. Hydrol.*,  
14 258(1-4), 214–231, doi:10.1016/S0022-1694(01)00565-0, 2002.
- 15 Fekete, B. M. and Vörösmarty, C. J.: The current status of global river discharge monitoring  
16 and potential new technologies complementing traditional discharge measurements, *Predict.*  
17 *Ungauged Basins PUB Kick-off (Proceedings PUB Kick-off Meet. held Bras. Novemb. 2002)*,  
18 *IAHS Publ. no. 309*, 129–136, 2007.
- 19 Global Runoff Data Centre: Major River Basins of the World / Global Runoff Data Centre,  
20 Koblenz, Germany: Federal Institute of Hydrology (BfG). [online] Available from:  
21 <http://grdc.bafg.de>, 2007.
- 22 Guha-Sapir, D., Hoyois, P. and Below, R.: *Annual Disaster Statistical Review 2013: The*  
23 *Numbers and Trends*, Brussels: CRED., 2014.
- 24 Haines, a. T., Finlayson, B. L. and McMahon, T. a.: A global classification of river regimes,  
25 *Appl. Geogr.*, 8(4), 255–272, doi:10.1016/0143-6228(88)90035-5, 1988.
- 26 Herdies, D. L.: Moisture budget of the bimodal pattern of the summer circulation over South  
27 America, *J. Geophys. Res.*, 107(D20), 8075, doi:10.1029/2001JD000997, 2002.
- 28 Hodgkins, G. ., Dudley, R. . and Huntington, T. .: Changes in the timing of high river flows in  
29 New England over the 20th Century, *J. Hydrol.*, 278(1-4), 244–252, doi:10.1016/S0022-  
30 1694(03)00155-0, 2003.
- 31 Hodgkins, G. a. and Dudley, R. W.: Changes in the timing of winter-spring streamflows in  
32 eastern North America, 1913-2002, *Geophys. Res. Lett.*, 33, 1–5, doi:10.1029/2005GL025593,  
33 2006.
- 34 ICOLD (International Commission on Large Dams): *World Register of Dams. Version*  
35 *updates 1998-2009*, Paris: ICOLD. [online] Available from: [www.icold-cigb.net](http://www.icold-cigb.net), 2009.

- 1 Javelle, P., Ouarda, T. B. M. J. and Bobée, B.: Spring flood analysis using the flood-duration-  
2 frequency approach: application to the provinces of Quebec and Ontario, Canada, *Hydrol.*  
3 *Process.*, 17(18), 3717–3736, doi:10.1002/hyp.1349, 2003.
- 4 Lehner, B., Liermann, C. R., Revenga, C., Vörösmarty, C., Fekete, B., Crouzet, P., Döll, P.,  
5 Endejan, M., Frenken, K., Magome, J., Nilsson, C., Robertson, J. C., Rödel, R., Sindorf, N.  
6 and Wisser, D.: High-resolution mapping of the world's reservoirs and dams for sustainable  
7 river-flow management, *Front. Ecol. Environ.*, 9(9), 494–502, doi:10.1890/100125, 2011.
- 8 Lima, K. C. and Satyamurty, P.: Post-summer heavy rainfall events in Southeast Brazil  
9 associated with South Atlantic Convergence Zone, *Atmos. Sci. Lett.*, 11(1), n/a–n/a,  
10 doi:10.1002/asl.246, 2010.
- 11 McCabe, G. J. and Wolock, D. M.: Joint Variability of Global Runoff and Global Sea Surface  
12 Temperatures, *J. Hydrometeorol.*, 9(4), 816–824, doi:10.1175/2008JHM943.1, 2008.
- 13 McMahon, T. A.: *Global runoff: continental comparisons of annual flows and peak discharges*,  
14 Catena Verlag, Cremlingen-Destedt, Germany., 1992.
- 15 McMahon, T. a., Vogel, R. M., Peel, M. C. and Pegram, G. G. S.: Global streamflows – Part 1:  
16 Characteristics of annual streamflows, *J. Hydrol.*, 347(3-4), 243–259,  
17 doi:10.1016/j.jhydrol.2007.09.002, 2007.
- 18 Milly, P. C. D., Dunne, K. a and Vecchia, a V: Global pattern of trends in streamflow and  
19 water availability in a changing climate, *Nature*, 438(7066), 347–350,  
20 doi:10.1038/nature04312, 2005.
- 21 Mishra, A. K., Singh, V. P. and Özger, M.: Seasonal streamflow extremes in Texas river  
22 basins: Uncertainty, trends, and teleconnections, *J. Geophys. Res. Atmos.*, 116(8), 1–28,  
23 doi:10.1029/2010JD014597, 2011.
- 24 Munich Re: *Topics Geo 2012 Issue. Natural Catastrophes 2011. Analyses, Assessments,*  
25 *Positions*, Münchener Rückversicherungs-Gesellschaft, Munich., 2012.
- 26 Peel, M. C., McMahon, T. a. and Finlayson, B. L.: Continental differences in the variability of  
27 annual runoff-update and reassessment, *J. Hydrol.*, 295(1-4), 185–197,  
28 doi:10.1016/j.jhydrol.2004.03.004, 2004.
- 29 Peel, M. C., McMahon, T. A., Finlayson, B. L. and Watson, F. G. R.: Identification and  
30 explanation of continental differences in the variability of annual runoff, *J. Hydrol.*, 250(1-4),  
31 224–240, doi:10.1016/S0022-1694(01)00438-3, 2001.
- 32 Poff, N. L., Olden, J. D., Pepin, D. M. and Bledsoe, B. P.: Placing global stream flow  
33 variability in geographic and geomorphic contexts, *River Res. Appl.*, 22(2), 149–166,  
34 doi:10.1002/rra.902, 2006.
- 35 Probst, J. L. and Tardy, Y.: Long range streamflow and world continental runoff fluctuations  
36 since the beginning of this century, *J. Hydrol.*, 94(3-4), 289–311, doi:10.1016/0022-  
37 1694(87)90057-6, 1987.

- 1 Seleshi, Y. and Zanke, U.: Recent changes in rainfall and rainy days in Ethiopia, *Int. J.*  
2 *Climatol.*, 24(8), 973–983, doi:10.1002/joc.1052, 2004.
- 3 Smith, R. L.: Threshold Methods for Sample Extremes, in *Statistical Extremes and*  
4 *Applications*, pp. 621–638, D. Reidel, Dordrech, Netherlands., 1984.
- 5 Smith, R. L.: Estimating Tails of Probability Distributions, *Ann. Stat.*, 15(3), 1174–1207,  
6 doi:10.1214/aos/1176350499, 1987.
- 7 Todorovic, P. and Zelenhasic, E.: A Stochastic Model for Flood Analysis, *Water Resour. Res.*,  
8 6(6), 1641–1648, doi:10.1029/WR006i006p01641, 1970.
- 9 UNISDR: Global Assessment Report on Disaster Risk Reduction (GAR 11) - Revealing Risk,  
10 Redefining Development, Geneva, Switzerland: United Nations Office for Disaster Risk  
11 Reduction (UNISDR)., 2011.
- 12 Uppala, S. M., KÅllberg, P. W., Simmons, a. J., Andrae, U., Bechtold, V. D. C., Fiorino, M.,  
13 Gibson, J. K., Haseler, J., Hernandez, A., Kelly, G. a., Li, X., Onogi, K., Saarinen, S., Sokka,  
14 N., Allan, R. P., Andersson, E., Arpe, K., Balmaseda, M. a., Beljaars, a. C. M., Berg, L. Van  
15 De, Bidlot, J., Bormann, N., Caires, S., Chevallier, F., Dethof, A., Dragosavac, M., Fisher, M.,  
16 Fuentes, M., Hagemann, S., Hólm, E., Hoskins, B. J., Isaksen, L., Janssen, P. a. E. M., Jenne,  
17 R., McNally, a. P., Mahfouf, J.-F., Morcrette, J.-J., Rayner, N. a., Saunders, R. W., Simon, P.,  
18 Sterl, A., Trenberth, K. E., Untch, A., Vasiljevic, D., Viterbo, P. and Woollen, J.: The ERA-  
19 40 re-analysis, *Q. J. R. Meteorol. Soc.*, 131(612), 2961–3012, doi:10.1256/qj.04.176, 2005.
- 20 Visser, H., Petersen, A. C. and Ligtoet, W.: On the relation between weather-related disaster  
21 impacts, vulnerability and climate change, *Clim. Change*, 461–477, doi:10.1007/s10584-014-  
22 1179-z, 2014.
- 23 Wada, Y., van Beek, L. P. H., Viviroli, D., Dürr, H. H., Weingartner, R. and Bierkens, M. F.  
24 P.: Global monthly water stress: 2. Water demand and severity of water stress, *Water Resour.*  
25 *Res.*, 47(7), n/a–n/a, doi:10.1029/2010WR009792, 2011.
- 26 Wang, B.: Climatic Regimes of Tropical Convection and Rainfall, *J. Clim.*, 7(7), 1109–1118,  
27 doi:10.1175/1520-0442(1994)007<1109:CROTCA>2.0.CO;2, 1994.
- 28 Ward, P. J., Eisner, S., Flörke, M., Dettinger, M. D. and Kummu, M.: Annual flood  
29 sensitivities to El Niño–Southern Oscillation at the global scale, *Hydrol. Earth Syst. Sci.*,  
30 18(1), 47–66, doi:10.5194/hess-18-47-2014, 2014.
- 31 Ward, P. J., Jongman, B., Weiland, F. S., Bouwman, A., van Beek, R., Bierkens, M. F. P.,  
32 Ligtoet, W. and Winsemius, H. C.: Assessing flood risk at the global scale: Model setup,  
33 results, and sensitivity, *Environ. Res. Lett.*, 8(4), 44019, doi:10.1088/1748-9326/8/4/044019,  
34 2013.
- 35 WCD (World Commission on Dams): Dams and development: a framework for decision  
36 making, London, UK: Earthscan., 2000.

- 1 Weedon, G. P., Gomes, S., Viterbo, P., Shuttleworth, W. J., Blyth, E., Österle, H., Adam, J. C.,  
2 Bellouin, N., Boucher, O. and Best, M.: Creation of the WATCH Forcing Data and Its Use to  
3 Assess Global and Regional Reference Crop Evaporation over Land during the Twentieth  
4 Century, *J. Hydrometeorol.*, 12(5), 823–848, doi:10.1175/2011JHM1369.1, 2011.
- 5 Winsemius, H. C., Van Beek, L. P. H., Jongman, B., Ward, P. J. and Bouwman, a.: A  
6 framework for global river flood risk assessments, *Hydrol. Earth Syst. Sci.*, 17(5), 1871–1892,  
7 doi:10.5194/hess-17-1871-2013, 2013.
- 8 Woodhouse, C. A.: Winter climate and atmospheric circulation patterns in the Sonoran desert  
9 region, USA, *Int. J. Climatol.*, 17(8), 859–873, doi:10.1002/(SICI)1097-  
10 0088(19970630)17:8<859::AID-JOC158>3.0.CO;2-S, 1997.

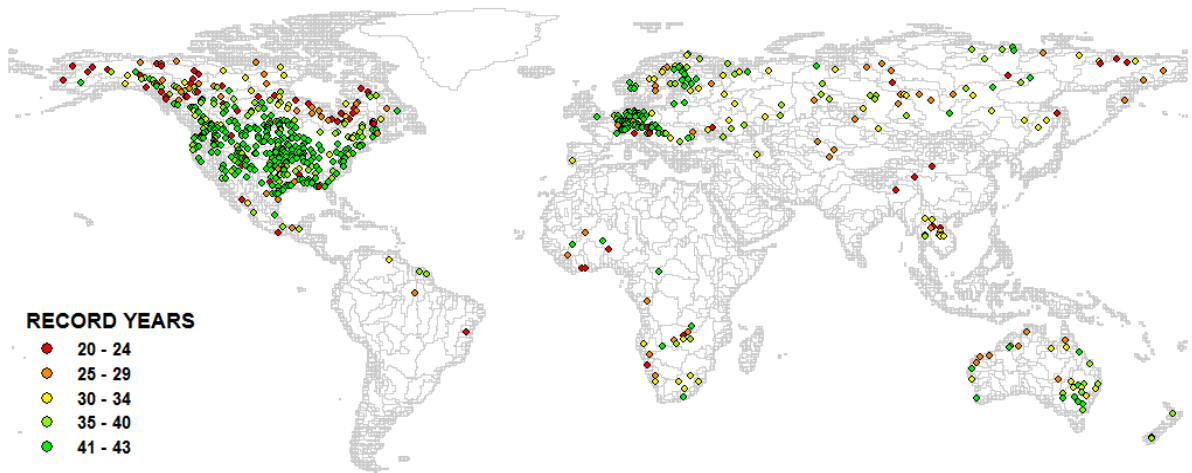
- 1 Table 1. Cross-correlations of Peak Month (PM) at GRDC stations for each classification
- 2 technique for (a) observed and (b) simulated streamflow.

Classification Technique		5% Threshold	Q <sub>AMF</sub>	Q <sub>7day</sub>	Q <sub>15day</sub>	Q <sub>30day</sub>
Observed	5% Threshold	1				
	Q <sub>AMF</sub>	0.866	1			
	Q <sub>7day</sub>	0.894	0.912	1		
	Q <sub>15day</sub>	0.895	0.880	0.945	1	
	Q <sub>30day</sub>	0.900	0.832	0.881	0.890	1
Simulated	5% Threshold	1				
	Q <sub>AMF</sub>	0.849	1			
	Q <sub>7day</sub>	0.873	0.926	1		
	Q <sub>15day</sub>	0.884	0.912	0.940	1	
	Q <sub>30day</sub>	0.888	0.880	0.902	0.911	1

1 Table 2. Comparison of Peak Month (PM) for flooding and calculated  $P_{AMF}$  at 6 GRDC stations in the Zambezi River Basin.

Station (GRDC sta. numb.)	STA01 (1591001)		STA02 (1291100)		STA03 (1591406)		STA04 (1591404)		STA05 (1591403)		STA06 (1591401)		Final PM
Station name	Senanga		Katima Mulilo		Machiya Ferry		Kafue Hook Bridge		Itezhi-Tezhi		Kasaka		
River name	Zambezi		Zambezi		Kafue		Kafue		Kafue		Kafue		
Cumulative catchment area ( $km^2$ )	284,538		339,521		23,065		96,239		105,672		153,351		
Mean annual streamflow ( $m^3/s$ )	975		1168		139		287		353		988		
Streamflow type	Natural		Natural		Natural		Natural		Natural (Reservoir inflow)		Regulated		
Classification Technique	PM (month)	PAMF (%)	PM (month)	PAMF (%)	PM (month)	PAMF (%)	PM (month)	PAMF (%)	PM (month)	PAMF (%)	PM (month)	PAMF (%)	
Observed	4	96	4	100	3	93	3	100	3	94	7	36	3
Simulated	3	100	3	97	2	97	3	75	2	94	2	97	2

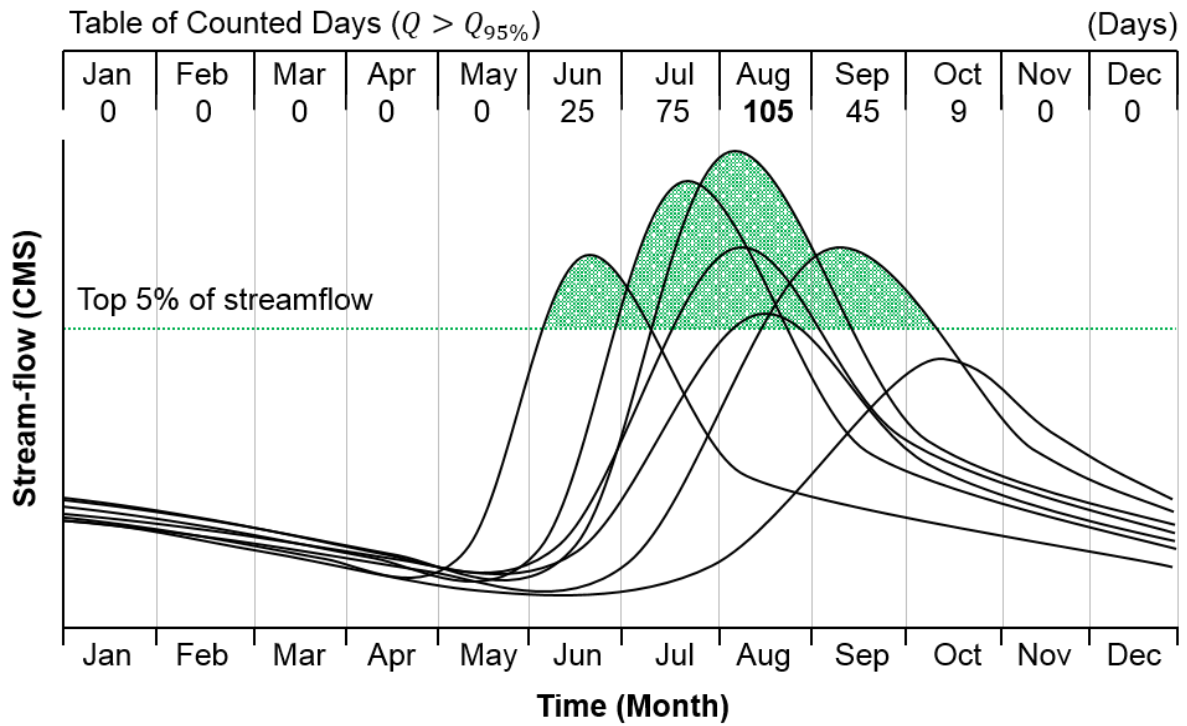
2



1

2 Figure 1. Location of 691 selected GRDC stations with corresponding number of years per  
3 station. Background polygons are world sub-basins based on 30' drainage direction maps  
4 ([Döll and Lehner, 2002](#)) with separation of large basins ([Ward et al., 2014](#)).

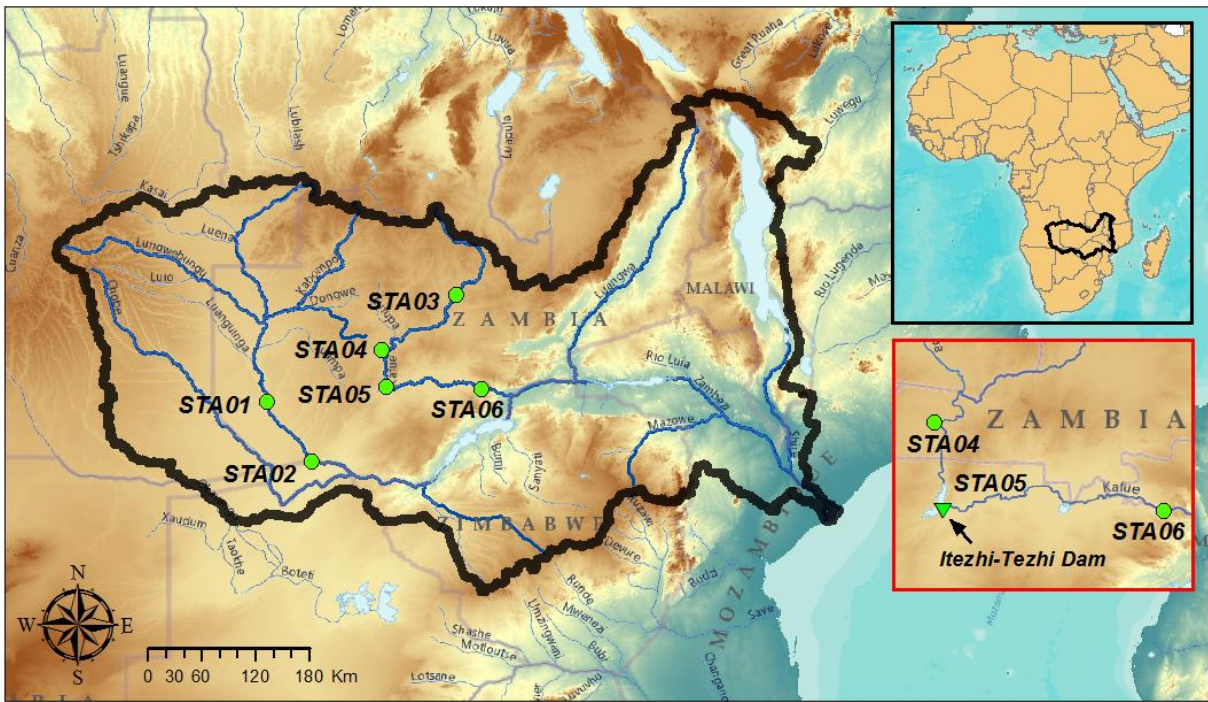




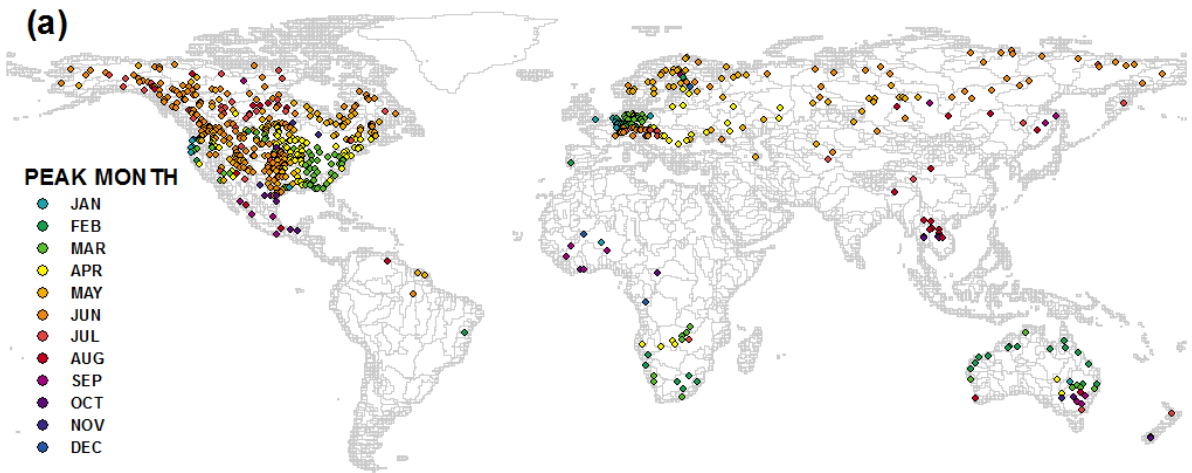
1

2 Figure 2. Seven years of synthetic streamflow data. Dotted line represents the 5% streamflow

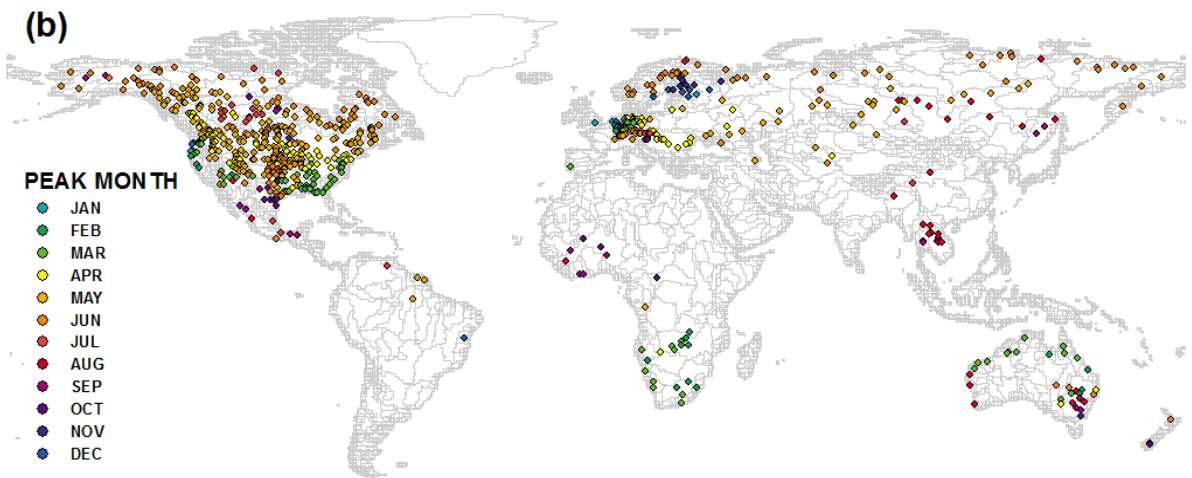
3 threshold. Numbers indicates the total days above the threshold for each month.



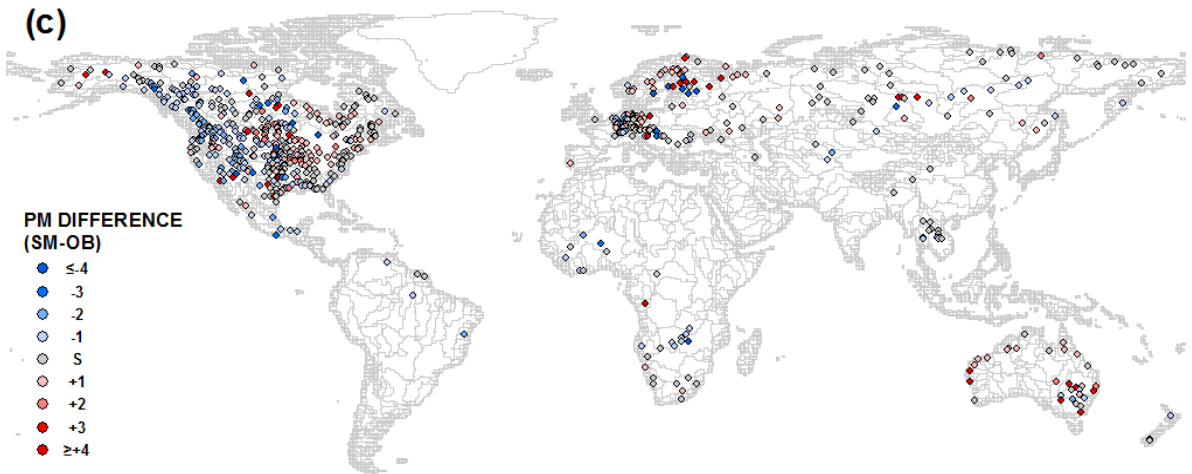
1  
 2 Figure 3. Map of Zambezi River Basin; the solid black line delineates the basin and the green  
 3 points are the 6 GRDC stations (STA01-06), with STA06 downstream of the Itezhi-Tezhi dam  
 4 (STA05.)



1

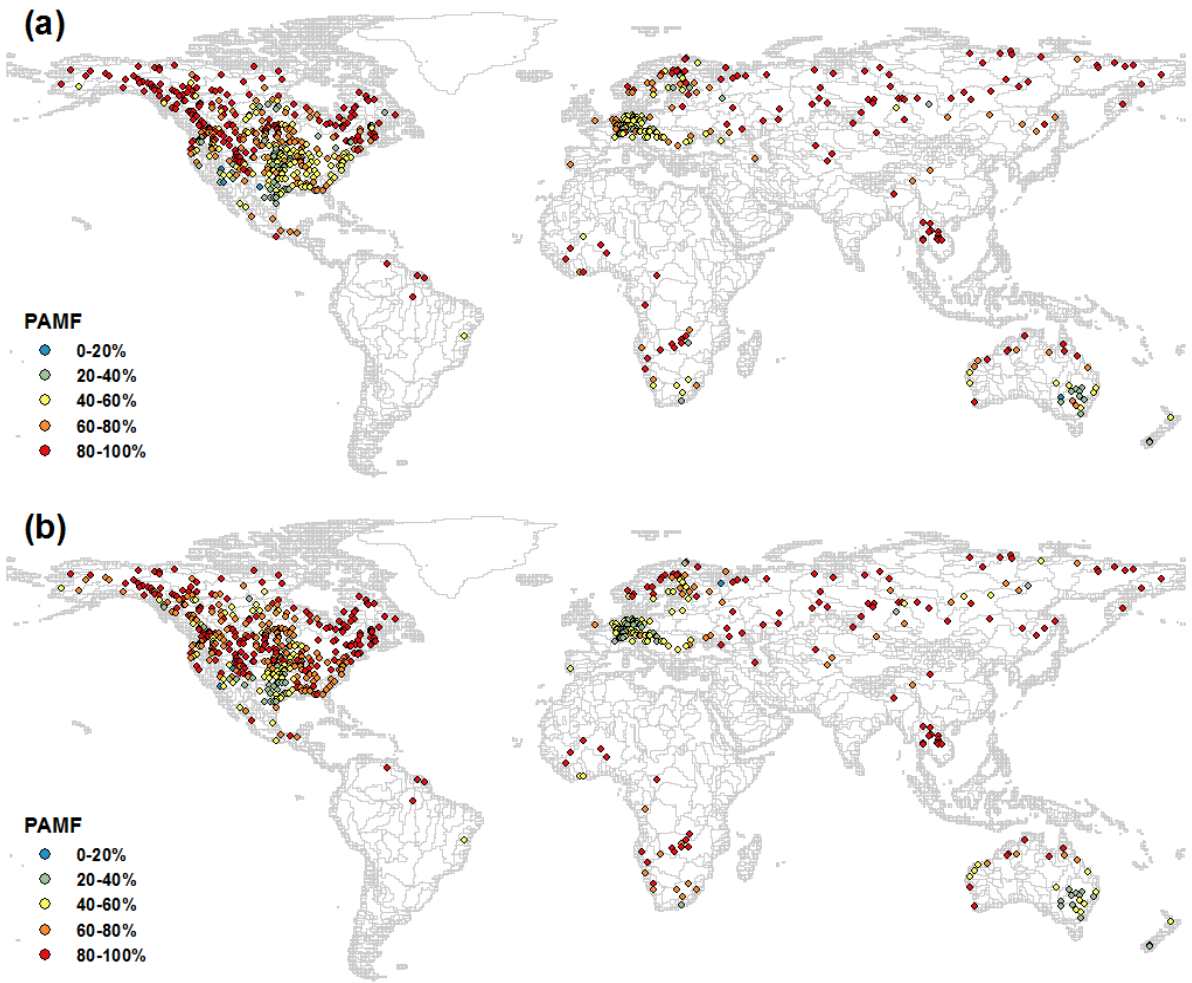


2



3

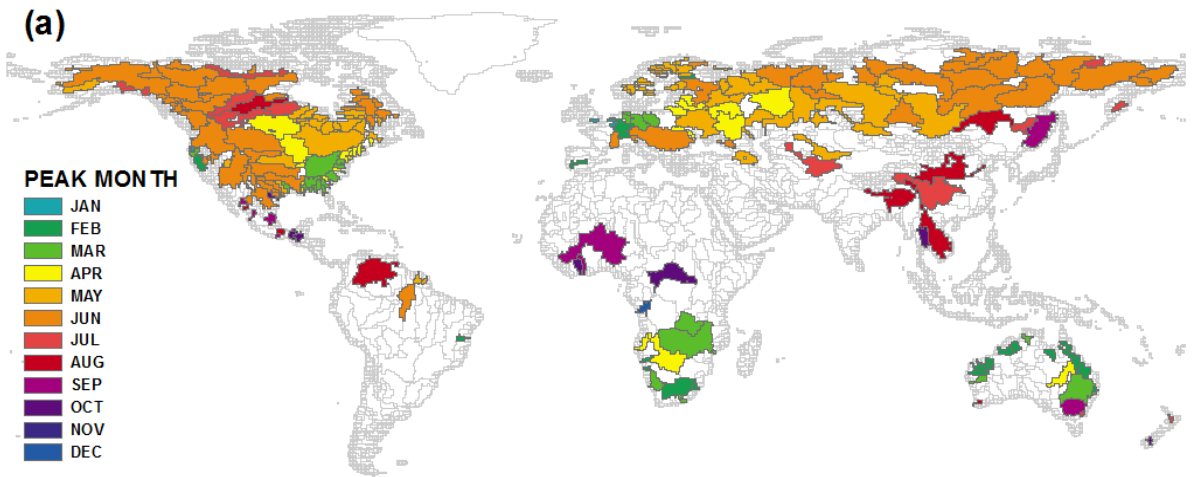
4 Figure 4. Peak Month (PM) for flooding as defined by (a) 691 GRDC observation stations, (b)  
 5 simulated streamflow at associated locations and (c) Temporal difference in PM between  
 6 observations and simulation (SM-OB, number of months).



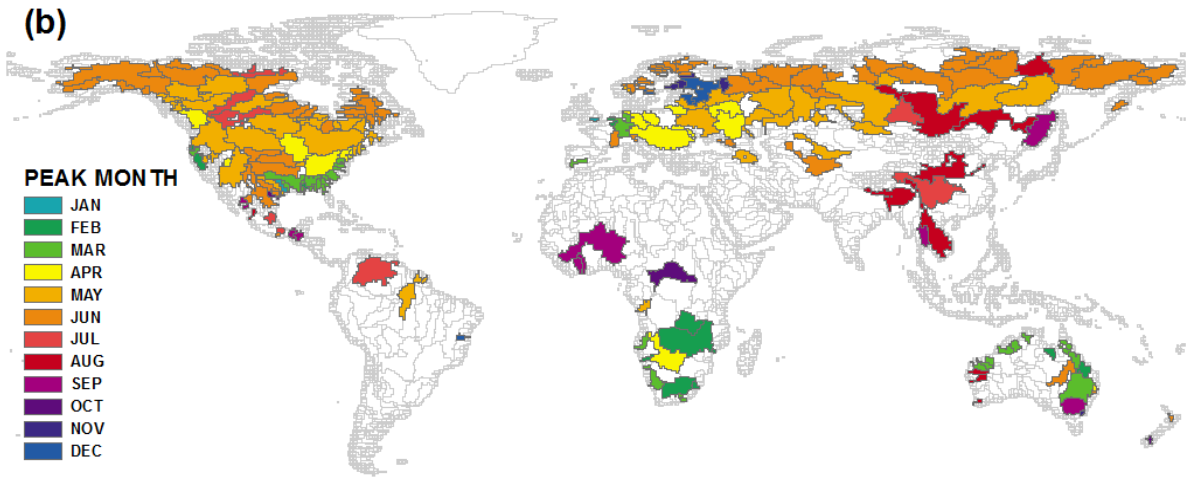
1

2

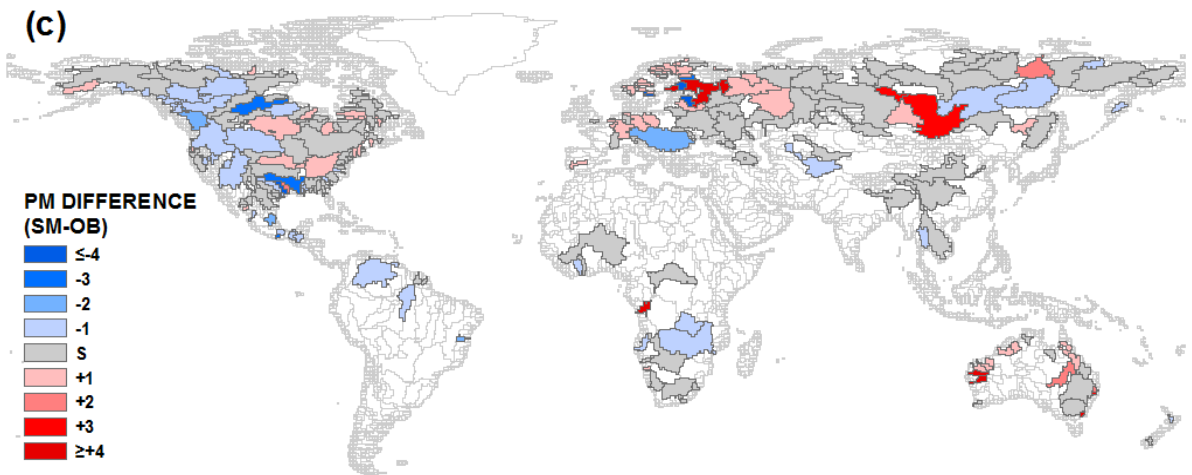
3 Figure 5. Calculated Percentage of Annual Maximum Flow (PAMF) values for (a) 691 GRDC  
 4 observation stations, and (b) simulated streamflow at associated locations.



1



2



3

4 Figure 6. Peak Month (PM) for flooding by sub-basin as defined by (a) 691 GRDC  
 5 observation stations, (b) simulated streamflow at associated sub-basins and (c) Temporal  
 6 difference in PM between observations and simulation (SM-OB, number of months).

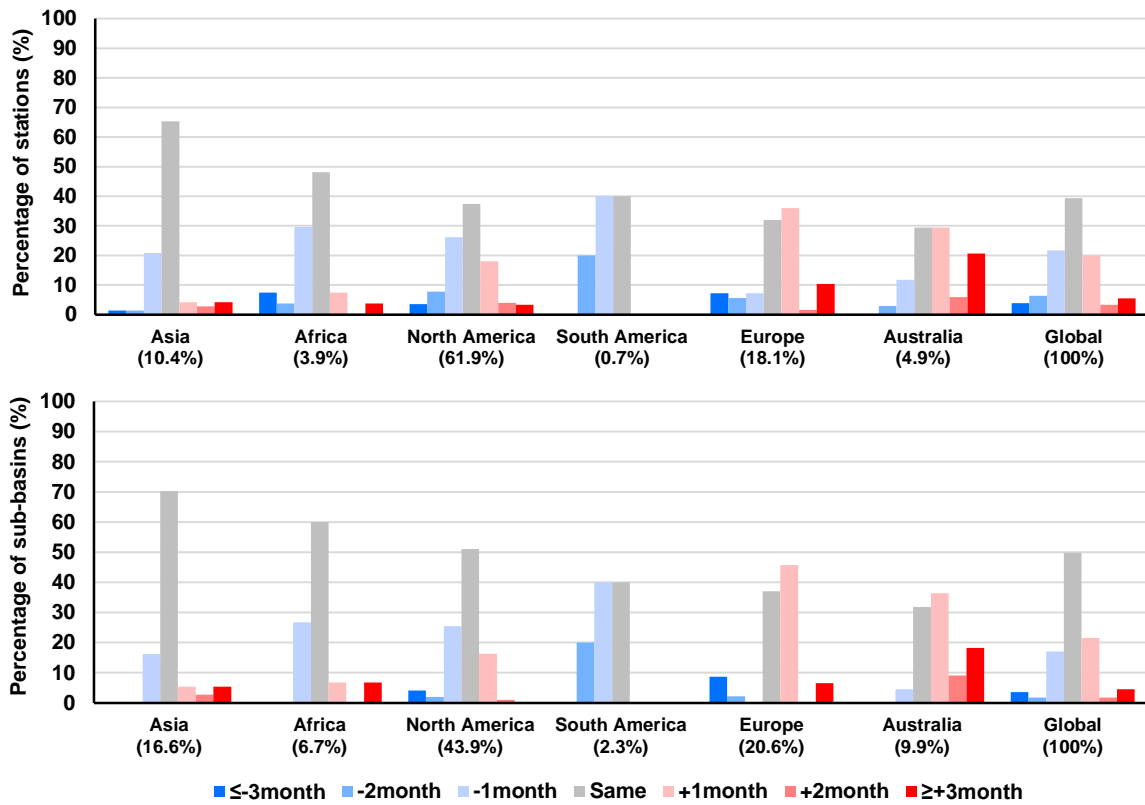
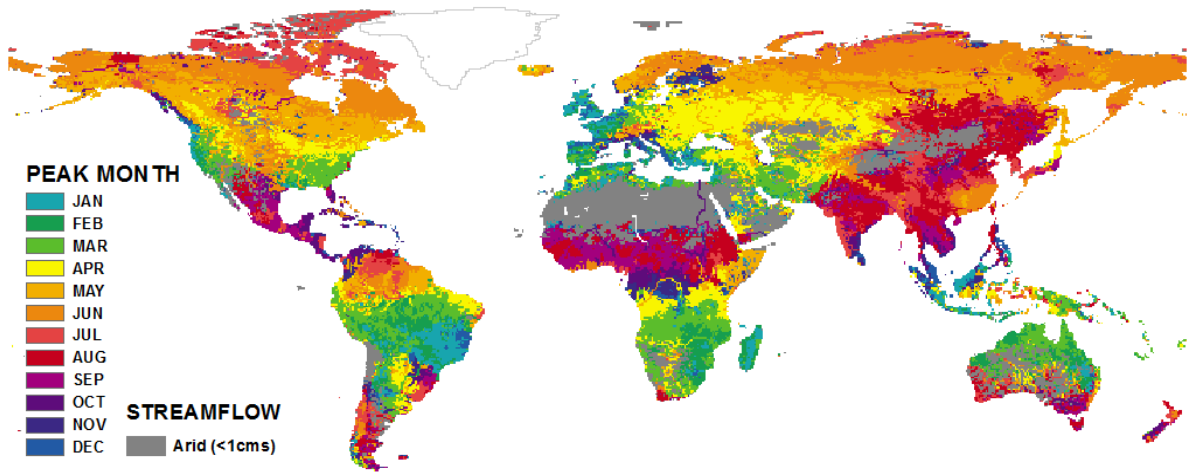
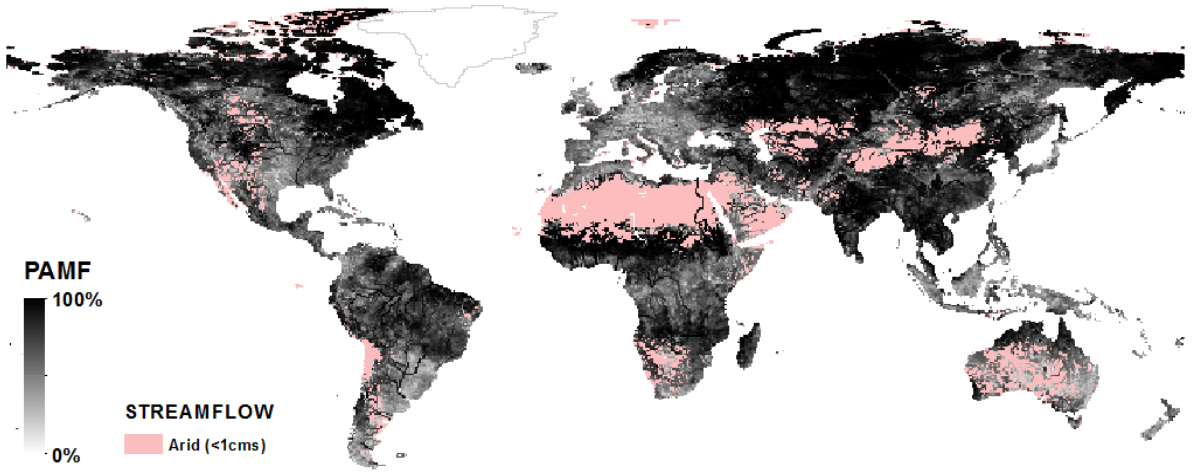


Figure 7. Percentage of stations (above) and sub-basins (below) according to temporal difference of PM between observations and model outputs (SM-OB, number of months) in each continent.



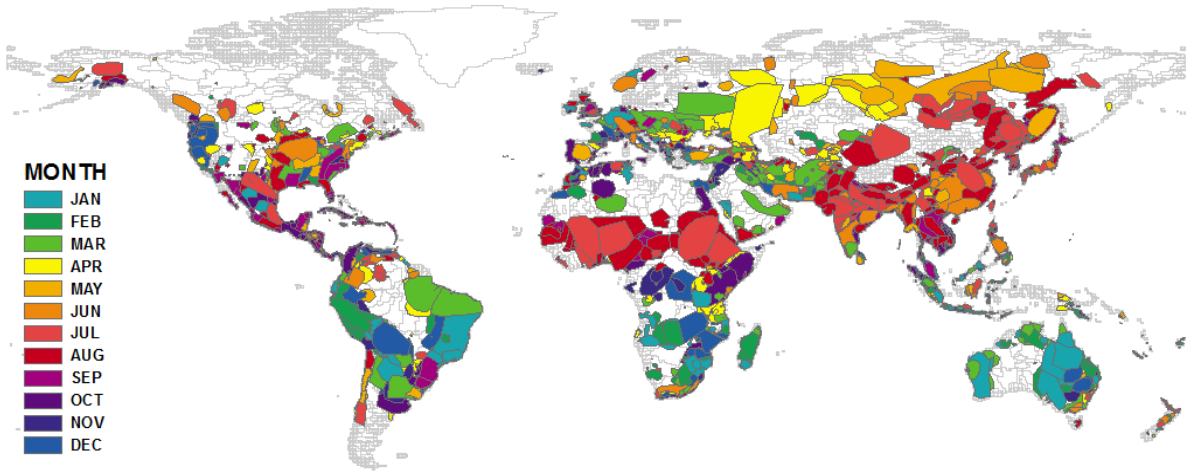
1

2 Figure 8. Peak Month (PM) for flooding as defined at all modeled grid cells.

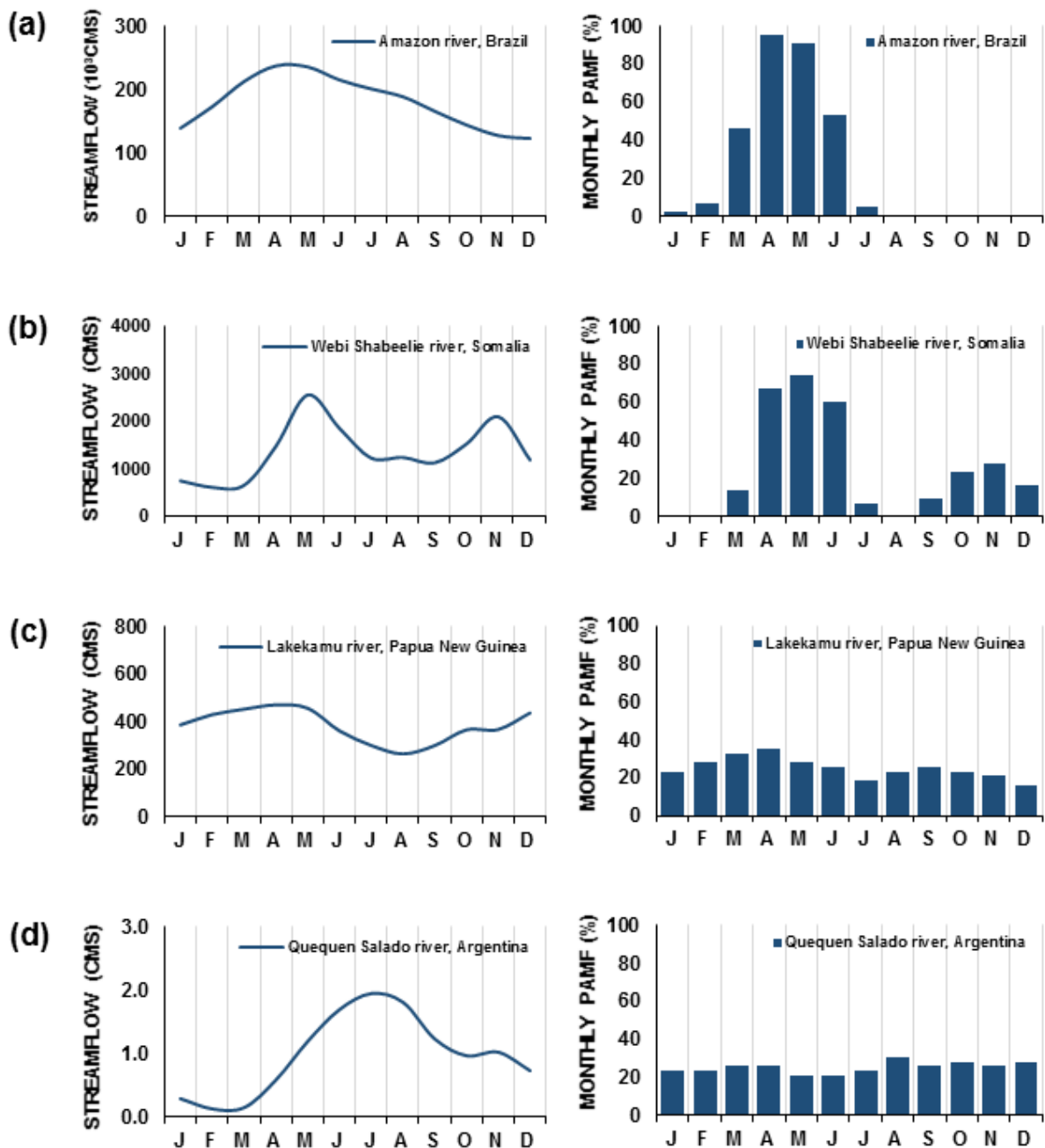


1  
2 Figure 9. Calculated Percentage of Annual Maximum Flow (PAMF) values for at all modeled  
3 grid cells.

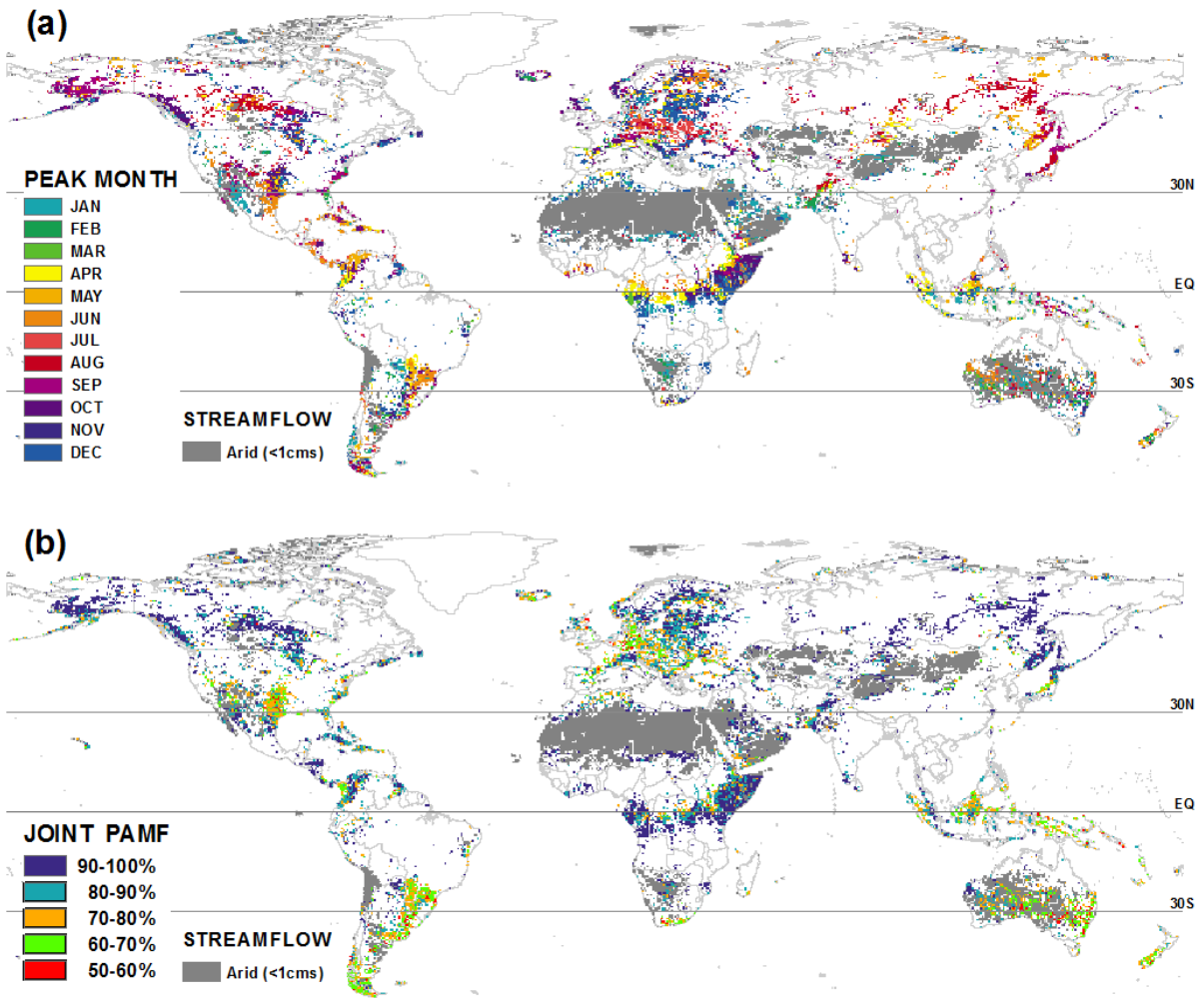




1  
2 Figure 10. Archive of major flood events globally from the Dartmouth Flood Observatory  
3 (DFO) over 1985-2008.



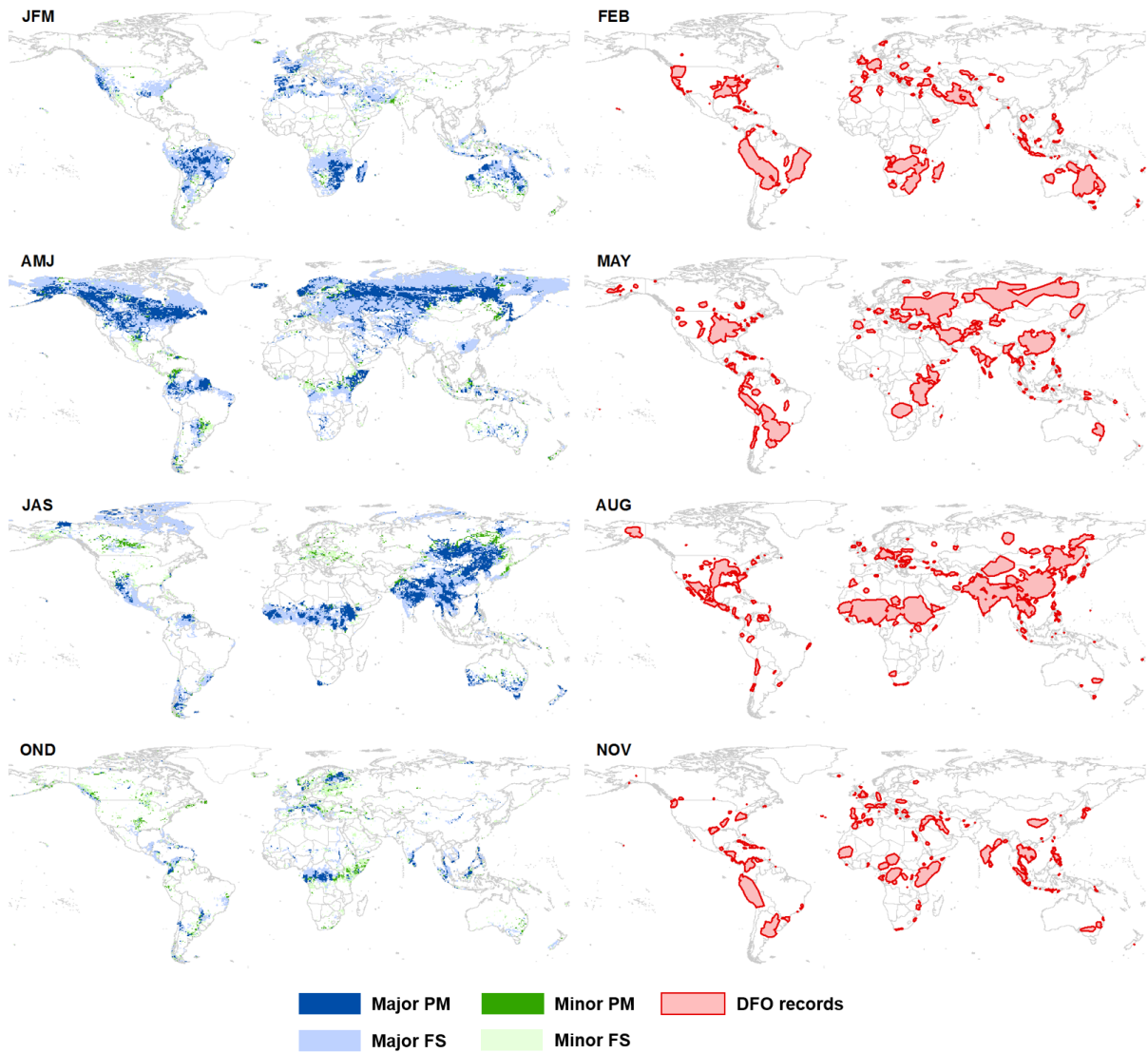
1  
2 Figure 11. Model-based streamflow climatology (left) and corresponding monthly PAMF  
3 (right.) Types and locations are: a) uni-modal streamflow – At Bom Lugar, Amazon river,  
4 Brazil, b) bimodal streamflow – At Saacow, Webi Shabeelie river, Somalia, c) constant  
5 streamflow – At Terapo Mission, Lakekamu river, Papua New Guinea and d) low-flow – At  
6 La Sortija, Quequen Salado river, Argentina.



1

2

3 Figure 12. (a) Minor Peak Month (PM) for flooding as defined at detected grid cells and (b)  
 4 joint PAMFs of major and minor PMs at corresponding cells.



1  
 2 Figure 13. Defined major FS and minor FS where joint PAMF is greater than 60% (left); peak  
 3 month of major and minor FSs (dense color) and pre- and post-month of major and minor FSs  
 4 (light color.) Monthly accumulated actual flood records (DFO) during 1958-2008 (right.)